Absence of receptor guanylyl cyclase C enhances ileal damage and reduces cytokine and antimicrobial peptide production during oral *Salmonella* Typhimurium infection

Shamik Majumdar[a], Vishwas Mishra[b], Somesh Nandi[b], Mudabir Abdullah[b], Anaxee Barman[b], Abinaya Raghavan[a], Dipankar Nandi[a] and Sandhya S. Visweswariah[b#]

Department of Biochemistry[a], Department of Molecular Reproduction, Development and Genetics[b], Indian Institute of Science, Bangalore, India.

Running Head: Guanylyl cyclase C and *Salmonella* infection

Keywords: *Salmonella* Typhimurium; guanylyl cyclase C; guanylin; uroguanylin; thymic atrophy; goblet cell

Address correspondence to Sandhya S. Visweswariah : sandhya@iisc.ac.in

SM, VM and SN contributed equally to this work

Abstract

Non-typhoidal *Salmonella* disease contributes towards significant morbidity and mortality across the world. Host factors including IFN-γ, TNF-α and gut microbiota, significantly influence the outcome of *Salmonella* pathogenesis. However, the entire repertoire of host protective mechanisms contributing to *Salmonella* pathogenicity is not completely appreciated. Here, we have investigated the roles of receptor guanylyl cyclase C (GC-C) that is predominantly expressed in the intestine, and regulates intestinal cell proliferation and fluid-ion homeostasis. Mice deficient in GC-C (*Gucy2c*$^{-/-}$) displayed accelerated mortality following infection via the oral route, in spite of possessing comparative systemic *Salmonella* infection burden. Survival following intra-peritoneal infection remained similar, indicating that GC-C offered protection via a gut-mediated response. Serum cortisol was higher in *Gucy2c*$^{-/-}$ mice, in comparison to wild type (*Gucy2c*$^{+/+}$) mice, and an increase in infection-induced thymic atrophy, with loss in immature $CD4^{+}CD8^{+}$ double positive thymocytes, was observed. Accelerated and enhanced damage in the ileum, including submucosal edema, epithelial cell damage, focal tufting and distortion of villus architecture, was seen in *Gucy2c*$^{-/-}$ mice, concomitant with a larger number of ileal tissue-associated bacteria. Transcription of key mediators in *Salmonella*-induced inflammation (IL-22/Reg3β) were altered in *Gucy2c*$^{-/-}$ mice in comparison to *Gucy2c*$^{+/+}$ mice. A reduction in fecal Lactobacilli, which are protective against Salmonella infection, was observed in *Gucy2c*$^{-/-}$ mice. *Gucy2c*$^{-/-}$ mice co-housed with wild type mice continued to show reduced Lactobacilli and increased susceptibility to infection. Our study therefore suggests that receptor GC-C confers a survival advantage during gut-mediated *S.* Typhimurium pathogenesis, presumably by regulating *Salmonella*-effector mechanisms and maintaining a beneficial microbiome.

Introduction

Salmonellosis, the disease caused by the Gram-negative intracellular bacterium, *Salmonella* manifests in humans as typhoid, paratyphoid fever, non-typhoidal septicemia or gastroenteritis. Infection with *Salmonella* Typhi and Paratyphi serotypes are limited to humans, and cause the systemic disease, typhoid fever. Infections with other serotypes, called non-typhoidal *Salmonella*, result in enteritis and diarrhoea. *Salmonella* infects hosts orally via contaminated food or water (1). Mice infection models are useful not only to study factors in the pathogen that regulate disease progression, but also host factors that can modulate the severity of response to *Salmonella* infection (2). In susceptible mouse strains, such as those with defects in the gene encoding Slc11a1 (Nramp1), the bacterium traverses the distal ileum, and mice develop systemic infection after colonizing the Peyer's patches, liver and spleen (3).

Colonization of the mouse intestine is dependent on a number of factors, that include commensal microbiota, the gut mucosa and the gut-associated immune system. A number of host factors such as IFN-γ (4), TNF-α (5, 6) and IL-22 modulate *Salmonella* pathogenesis (1). These factors regulate the production of chemokines that recruit inflammatory cells to the site of tissue damage and infection (7). In addition, it is conceivable that modulators of intestinal epithelial cell function may also provide mechanisms to modulate *Salmonella* pathogenesis, since the first point of contact for the pathogen is the epithelial cells that line the gastrointestinal tract (8).

Receptor guanylyl cyclase C (GC-C) is a transmembrane receptor predominantly expressed on the apical membrane of the intestinal enterocytes. It serves as a receptor for the endogenous hormones, guanylin and uroguanylin (9, 10). Activation of GC-C upon ligand-binding results in production of cGMP, which leads to protein kinase G II-dependent

activation of the cystic fibrosis transmembrane conductance regulator (CFTR) and inhibition of NHE3, the sodium–hydrogen exchanger 3. Activation of CFTR causes efflux of chloride and CFTR-dependent bicarbonate secretion into the lumen and inhibition of sodium absorption by NHE3, thus resulting in an osmotic gradient, leading to fluid accumulation in the lumen. Hence, the major role of GC-C is in maintenance of fluid-ion homeostasis in the gut (11). GC-C also serves as the receptor for the heat-stable enterotoxin (ST), the causative agent of enterotoxigenic *Escherichia coli* (ETEC)-mediated diarrhoea in children and traveller's diarrhoea (12). Mice lacking GC-C are resistant to heat-stable enterotoxin-induced fluid accumulation (13), and are reported to display higher susceptibility to dextran sodium sulphate-induced colitis (14). Previously, we have demonstrated that mice lacking GC-C show increased N-Methyl-N-nitrosourea-induced aberrant crypt foci (15), indicating a role for GC-C in maintaining intestinal cell proliferation.

Mice deficient in GC-C (i.e., *Gucy2c*$^{-/-}$) mice have been reported to possess a compromised gut epithelial barrier which was attributed to the lower expression of tight junction proteins such as occludin, claudin 2 and claudin 4 (14). *Citrobacter rodentium* (*C. rodentium*), an enteric Gram-negative bacterium causes self-limiting infection in mice, and *Gucy2c*$^{-/-}$ mice are reported to be more susceptible to infection by them (16). Here, we have studied the role of GC-C as a host factor during *Salmonella*-mediated pathogenesis in mice. We find that in contrast to expectations that a compromised gut barrier would lead to enhanced systemic infection, the increased susceptibility of *Gucy2c*$^{-/-}$ mice to oral infection with *Salmonella* Typhimurium (*S.* Typhimurium; St) was a result of increased bacterial load in the ileum, altered cytokine production, increased ileal tissue damage, and coupled to an altered fecal microbiome.

Results

Mice lacking GC-C display accelerated mortality during oral *S.* Typhimurium infection

We infected C57BL/6 wild type (*Gucy2c*$^{+/+}$) and *Gucy2c*$^{-/-}$ mice orally with *S.* Typhimurium and monitored their survival. We chose not to treat the mice with streptomycin (17), since we were interested in an acute model of *S.* Typhimurium infection, without altering the existing microbiota in these mice (18). Surprisingly, survival experiments revealed an increased susceptibility of *Gucy2c*$^{-/-}$ mice to oral, but not intra-peritoneal, infection with *S.* Typhimurium (Fig. 1a), indicating a role for GC-C in offering protection to gut-associated infection. Median survival for *Gucy2c*$^{+/+}$ mice following oral infection was 112 h while it was 80 h for *Gucy2c*$^{-/-}$ mice, and the difference was statistically significant (p = 0.006). Interestingly, fecal excretion of bacteria was similar in *Gucy2c*$^{+/+}$ and *Gucy2c*$^{-/-}$ mice at early stages of infection, as was the bacterial burden in organs such as the spleen, Peyer's patches and liver on day 3 post infection (Fig. 1b, c). In agreement with earlier observations (19), poor survival on *Salmonella* infection was correlated with a significant reduction in body weight of *Gucy2c*$^{-/-}$ mice on day 3 (Fig. 1d).

Next, we monitored pro-inflammatory cytokines in the sera 3 days post oral infection, to determine whether enhanced immune cell activation and inflammation was responsible for the poor survival of *Gucy2c*$^{-/-}$ mice. As shown in Fig. 1e, while there was a tendency for an increase in serum TNF-α and IL-6 levels on infection, the increase was not statistically significant. IFN-γ levels were elevated on infection in both strains of mice, but there was no difference between *Gucy2c*$^{+/+}$ and *Gucy2c*$^{-/-}$ mice. Therefore, we conclude that an increase in systemic infection or inflammation was not the cause for early death of *Gucy2c*$^{-/-}$ mice.

Enhanced infection-induced thymic atrophy is observed in *Gucy2c*$^{-/-}$ mice

We have previously reported that serum cortisol, a marker of general stress experienced by the animal, is increased on *Salmonella* infection and contributes towards *S.* Typhimurium-induced thymic atrophy in mice (20, 21). We monitored cortisol levels and observed an

116 increase in serum cortisol on infection. However, at 48 h, *Gucy2c*$^{-/-}$ mice showed higher
117 levels of circulating cortisol than that seen in *Gucy2c*$^{+/+}$ mice (Fig. 2a). Thymic atrophy was
118 observed in both *Gucy2c*$^{+/+}$ and *Gucy2c*$^{-/-}$ mice (Fig. 2b, c), but was more pronounced in
119 *Gucy2c*$^{-/-}$ mice, both at 48 and 96 h post infection (Fig. 2b). CD4 and CD8 cell surface
120 staining of isolated thymocytes revealed an increased depletion of CD4^{+}CD8^{+} thymocytes in
121 *Gucy2c*$^{-/-}$ mice post 96 hrs of infection (Fig. 2c).

122 **Increased epithelial damage in the small intestine is observed in *Gucy2c*$^{-/-}$ mice**

123 Results so far suggest that the protective effects of GC-C are mediated predominantly at the
124 level of the gastrointestinal tract, and could be initiated early during infection, thereby
125 resulting in significant weight loss and earlier death in *Gucy2c*$^{+/+}$ mice. We therefore
126 monitored bacterial load in various regions of the gut following infection in both *Gucy2c*$^{+/+}$
127 and *Gucy2c*$^{-/-}$mice. Colony forming units (CFU) were enumerated on day 3 following
128 infection, at which time a few *Gucy2c*$^{-/-}$ mice had already succumbed. As shown in Fig. 3a,
129 while bacterial loads in the cecum and colon were similar in both strains of mice, and an
130 almost 2-log order increase in bacteria was seen in the distal ileum.

131 We measured ileal damage and goblet cell number on day 3, using Periodic Acid Schiff
132 (PAS) staining following paraformaldehyde fixation. Examination of small intestinal sections
133 showed marked histopathological differences between infected *Gucy2c*$^{+/+}$and *Gucy2c*$^{-/-}$ mice.
134 Infection resulted in more severe inflammation in the small intestine of *Gucy2c*$^{-/-}$ mice, with
135 increased focal tufting and distortion of the crypt-villus architecture by day 4 (Fig. 3b). A
136 larger number of dead cells were also observed in the lumen of the ileum in *Gucy2c*$^{-/-}$ mice by
137 day 4 post-infection.

138 PAS staining revealed a reduced number of goblet cells in uninfected *Gucy2c*$^{-/-}$ mice (Fig.
139 3c). Goblet cell numbers reduced in *Gucy2c*$^{+/+}$ on infection, as has been reported earlier

(17), but were increased in *Gucy2c*$^{-/-}$ mice. Also noteworthy is the intense staining of Paneth cells in the crypts of both *Gucy2c*$^{+/+}$ and *Gucy2c*$^{-/-}$ mice following infection.

_S_. Typhimurium infection downregulates the transcription of GC-C and its ligands, guanylin and uroguanylin

Results so far indicate that signaling via GC-C protects the host during *Salmonella* infection, by reducing the extent of tissue damage and colonization in the ileum. We therefore asked if infection alters the expression of genes in the GC-C signaling pathway, which could be a strategy used by *Salmonella* to increase its virulence in the host. We performed quantitative real-time PCR analysis of cDNA prepared from the distal ileum of *Gucy2c*$^{+/+}$ mice on day 3 following oral infection and observed that the transcript levels of GC-C were significantly reduced on infection (Fig. 4). The distal ileum may be a region where both guanylin and uroguanylin are expressed to comparable levels (22), and interestingly, transcript levels of both the ligands were reduced on infection in both *Gucy2c*$^{+/+}$ and *Gucy2c*$^{-/-}$ mice (Fig. 4). Other genes downstream of GC-C did not show a change in expression levels (*Cftr*, *PkgII* and *Pde5*) on infection, while *Nhe3* transcripts were upregulated in both *Gucy2c*$^{+/+}$ and *Gucy2c*$^{-/-}$ infected mice. Activation of GC-C results in cGMP-dependent phosphorylation of NHE3 that inhibits this Na^+/H^+ exchanger (11, 23). Therefore, the downregulation of guanylin and uroguanylin transcripts, coupled with increased expression of *Nhe3* would enhance Na^+ uptake by the epithelial cells, possibly counteracting loss of this ion during *Salmonella*-induced diarrhea in humans.

GC-C regulates transcription of cytokines and effectors during *Salmonella* infection

Intestinal inflammation following *Salmonella* infection is a consequence of upregulation of pro-inflammatory genes including *TNF-α*, *Il-1β*, *Il-22*, *Il-6*, *Ifn-γ* (24) and genes expressing the C-type lectins *Reg3γ* and *Reg3β* (1). Transcripts of most cytokines were upregulated to

similar extents in both *Gucy2c*$^{+/+}$ and *Gucy2c*$^{-/-}$ mice following infection (Fig. 5). Transcript levels of only a few genes (*Il-22*, *Cxcl15* and *Reg3β* ; see green bars in Fig. 5) differed statistically between *Gucy2c*$^{+/+}$ and *Gucy2c*$^{-/-}$ mice following infection. While *lipocalin 2* transcripts were significantly increased in *Gucy2c*$^{-/-}$ mice, there was no statistical difference between levels in wild type and *Gucy2c*$^{-/-}$ mice following infection. In summary, this indicates a role for GC-C signaling in modulating specific arms of the *Salmonella*-induced immune response.

Reduced *Lactobacilli* in *Gucy2c*$^{-/-}$ mice may contribute to initial susceptibility of mice to *Salmonella* infection

The gut microbiota is known to influence infection progression by *Salmonella* (17, 18, 25, 26). We therefore monitored the major Phyla of bacteria present in the mouse gut, and also *Lactobacillus sp* which has been reported to protect from *Salmonella* infection (25–28). We prepared genomic DNA from stool samples from both *Gucy2c*$^{+/+}$ and *Gucy2c*$^{-/-}$ mice, and performed real-time PCR using universal and Phyla specific primers for the 16S rRNA genes. As shown in Fig. 6, while the major Phyla (Bacteriodetes and Firmicutes) were largely unchanged in both strains of mice, *Lactobacillus sp* were significantly reduced. Since *Lactobacilli* have been reported to attenuate the severity of salmonellosis in mice (25), we propose that the initial environment of the gut of *Gucy2c*$^{-/-}$ mice could have also contributed to initial infection and uptake of *S.* Typhimurium, culminating in the increased susceptibility of *Gucy2c*$^{-/-}$ mice to infection.

To ensure that alterations in the microbiome in *Gucy2c*$^{-/-}$ mice were directly a consequence of the absence of GC-C in the gut, we co-housed *Gucy2c*$^{-/-}$ mice at the time of weaning with adult wild type mice for 4 weeks. We then monitored major Phyla in the feces collected from co-housed mice. We continued to observe a similar composition of microbiota after co-

188 housing, including the lower levels of *Lactobacilli* in *Gucy2c*$^{-/-}$ mice (Fig. 6a). We infected
189 these co-housed *Gucy2c*$^{-/-}$ mice along with age-matched wild type mice, housed both strains
190 of mice together in multiple cages following infection, and monitored survival. In agreement
191 with earlier results, we saw dramatically poorer survival of *Gucy2c*$^{-/-}$ mice that were co-
192 housed with infected *Gucy2c*$^{+/+}$ mice following infection (Fig. 6a). Similar fecal bacterial
193 loads (Fig. 6b) were observed in all mice, but *Gucy2c*$^{-/-}$ mice showed a marked reduction in
194 body weight by day 3. Therefore, these co-housing experiments suggest that susceptibility of
195 *Gucy2c*$^{-/-}$ mice to *Salmonella* infection is caused by genetically-determined changes in gut
196 response and microbiome composition.

197 **Discussion**

198 GC-C-mediated cGMP pathways are essential regulators of intestinal homeostasis, including
199 fluid-ion secretion and cell proliferation(23). The role of GC-C in diarrhea caused by
200 enterotoxigenic *E. coli* that produce heat-stable enterotoxins is well established, since GC-C
201 serves as the receptor for the toxin (11). However, the roles of GC-C, if any, during severe
202 enteric infections, have not been investigated. Here we have utilized the *S.* Typhimurium
203 infection model in mice which results in an acute, progressive and lethal infection, to study
204 the contribution of GC-C during *Salmonella* pathogenesis. Our results show that GC-C
205 provides protection to oral *S.* Typhimurium infection, and absence of GC-C was correlated
206 with reduced ileal damage and changes in the levels of some cytokines and antimicrobial
207 peptides (AMPs) (1, 24) (Fig. 7). Interestingly, the rapid mortality seen in *Gucy2c*$^{-/-}$ mice was
208 not dependent on increased systemic infection, since bacteria colonized extra-intestinal tissue
209 to equivalent extents in both *Gucy2c*$^{+/+}$ and *Gucy2c*$^{-/-}$ mice.

210 Glucocorticoids (GCs) are steroid hormones which are secreted by the adrenal glands and
211 possess immunosuppressive properties. GCs are an indicator of stress (29) and are

upregulated during *S.* Typhimurium infection in mice (21). At 48 h post infection, serum cortisol levels in *Gucy2c*$^{-/-}$ mice were significantly higher than that seen in *Gucy2c*$^{+/+}$ mice. Thymic atrophy accompanies numerous infections and GCs contribute towards depletion of the developing $CD4^+CD8^+$ immature thymocytes during infections by pathogens such as *Listeria monocytogenes*, type A *Francisella tularensis*, *Trypanosoma cruzi* and *S.* Typhimurium (20, 21). Since *Gucy2c*$^{-/-}$ mice displayed early elevated levels of serum cortisol (Fig. 2a), infection-induced thymic atrophy in *Gucy2c*$^{-/-}$ mice was indeed observed to be significantly higher than in *Gucy2c*$^{+/+}$ mice.

Higher circulating cortisol could be attributed to enhanced colonization and inflammation in *Gucy2c*$^{-/-}$ mice, as evidenced by histopathology of the ileum. *S.* Typhimurium infection results in inflammation of the cecum and colon, with lower inflammation seen in the ileum of mice (30). Germ-free mice display higher ileal load than specific-pathogen-free mice when administered with similar doses of *S.* Typhimurium (31). The higher colonization in the ileum of *Gucy2c*$^{-/-}$ mice may be due to higher translocation or invasion of *Salmonella* in the gut of these mice. Interestingly during Crohn's disease, selective inflammation in the terminal ileum is observed (32) . In addition, the standard therapy for inflammatory bowel disease (IBD) is administration of corticosteroids, which facilitate immunosuppression (33). The elevated levels of cortisol observed in *Gucy2c*$^{-/-}$ mice during infection (Fig. 2a) might be a compensatory mechanism to reduce inflammation of the ileum.

Salmonella pathogenesis results in altered gene expression profile in the intestine (1). The transcript levels of GC-C and its endogenous ligands, guanylin and uroguanylin were downregulated upon infection in the ileum (Fig. 4). However, the transcript levels of other downstream effectors of the GC-C pathway such as *PkgII, Cftr and Pde5* were not differentially modulated post infection. NHE3 is an abundantly expressed Na^+/H^+ exchanger in the intestine (11, 34). There was a significant increase in the expression of NHE3 upon

infection, which occurred independently of the presence of GC-C. The significant increase in NHE3 transcript levels is counterintuitive, since there are reports of downregulation of NHE3 by pro-inflammatory cytokines such as IFN-γ and TNF-α, during EPEC infection and inflammatory bowel disease (34). Mechanisms that lead to transcriptional regulation of NHE3 upon *Salmonella* infection are unknown and warrant further investigation.

There are only two reports of disruption of GC-C signaling at both receptor and ligand levels, as we see here on *Salmonella* infection (Fig. 4). In ulcerative colitis patients, a severity-dependent downregulation in expression of GC-C, guanylin and uroguanylin in the colonic mucosa, is observed (35). GC-C and its ligands are also downregulated in inflamed colonic IBD mucosa of patients, (36) and in 2,4,6-trinitrobenzene sulphonic acid-induced colitis in rats (37). The significant downregulation of GC-C and its ligands upon *Salmonella* infection could therefore occur as a consequence of altered composition of the tissue following the inflammation induced by infection.

Salmonella infection and invasion of the intestine induce inflammatory responses including upregulation of pro-inflammatory cytokines (24). The induction of TNF-α in the gastrointestinal tract during *Salmonella* infection is well known (5, 6). Low amounts of TNF-α confer protection to mice towards *Salmonella* infection (38), while administration of higher doses causes extensive histopathological damage, organ dysfunction and death within minutes to hours due to respiratory arrest (39, 40). Following infection, there was no statistical difference between transcript levels of TNF-α in the ileum in wild type and *Gucy2c*$^{-/-}$ mice. TNF-α mediates the depletion of goblet cells during *S.* Typhimurium infection in mice, as pre-treatment with anti-TNFα antibody restores the goblet cell numbers and mucin profiles (6). We however see an increase in goblet cell numbers on infection in the small intestine in *Gucy2c*$^{-/-}$ mice, suggesting a novel means of regulating goblet cell number by GC-C.

A critical arm of the antimicrobial innate immune response is the production of epithelial cell-derived AMPs. This antimicrobial response is mediated via the IL-22 cytokine, which induces the expression of AMPs in the intestinal epithelial cells (1). IL-22 is produced by leukocytes such as T helper type 17 (T_H17) cells in response to IL-23 produced by infected dendritic cells and macrophages (41) and/or IL-6 produced by intestinal epithelial cells (42). AMPs induced by IL-22 include REG3β, REG3γ, lipocalin 2 and calprotectin. REG3β and REG3γ are bactericidal C-type lectins and eliminate Gram-positive bacteria (1, 43). Lipocalin 2 and calprotectin do not kill bacteria directly but starve them of metals which are essential for their growth (1). This AMP response has been demonstrated to impart a growth advantage to Gram-negative pathogens such as *Salmonella* over commensal bacteria (44). *Reg3γ*$^{-/-}$ and *Reg3β*$^{-/-}$ mice are more susceptible to *Salmonella enteritidis* infection, implying a protective role of these AMPs against this pathogen (45, 46). The lower infection-induced expression of IL-22 in *Gucy2c*$^{-/-}$ mice (Fig. 5) may affect the induction of AMPs in the epithelial cells, and indeed, the transcript levels of Reg3β in *Gucy2c*$^{-/-}$ mice were found to be significantly lower upon infection than in *Gucy2c*$^{+/+}$ mice. This may also partly account for the susceptibility of these mice to *Salmonella* infection.

Innate lymphoid cells are potent producers of IL-22 after intestinal injury. Importantly, IL-22 has been shown to induce intestinal epithelial regeneration, by increasing proliferation of intestinal stem cells (47). *Gucy2c*$^{-/-}$ mice showed a reduction in *Il-22* transcripts on infection (Fig. 6). It is possible that the increased intestinal damage seen in *Gucy2c*$^{-/-}$ mice could be a consequence of reduced proliferation of stem cells and therefore replenishment of epithelial cells.

The gastrointestinal tract is a rich source of aryl hydrocarbon receptor (AhR) ligands (48). Ahr protects the gut upon challenge with pathogenic bacteria (49)by increasing Il-22 expression. Thus, AhR-deficient mice succumb to *Citrobacter rodentium* infection, and

ectopic expression of IL-22 protected mice from this early mortality (49). It would therefore be of interest to monitor AhR expression in the gut of *Gucy2c*$^{-/-}$ mice and determine whether this contributes to reduced *Il-22* transcripts in infected mice.

The gut microbiota is a critical determinant for susceptibility to various infectious pathogens (50) including *S.* Typhimurium (17, 18, 25, 26). The gut microbiota can either promote resistance to colonization of pathogens or assist and enhance its virulence (50). In our study, there were no significant differences in the abundance of the major phyla (i.e., Bacteriodetes, Firmicutes, Actinobacteria and Proteobacteria) in *Gucy2c*$^{+/+}$ and *Gucy2c*$^{-/-}$ mice (Fig. 6a). However, we observed a significant decrease in the abundance of *Lactobacillus* in *Gucy2c*$^{-/-}$ mice, as has been reported earlier (16). We observed this decrease even following co-housing of *Gucy2c*$^{-/-}$ mice with wild type mice. (Fig. 6). Different species and isolates of *Lactobacillus* have been shown to exert antagonistic activity on Salmonella invasion and colonization (25–28). For example, *Lactobacillus acidophilus* inhibits adhesion, invasion and dissemination of attenuated *S.* Typhimurium in BALB/c mice (25). In vitro studies in human intestinal Caco-2 cells reveal that *Lactobacillus acidophilus* attenuates *Salmonella*-induced intestinal inflammation via transforming growth factor β/MIR21 signaling pathway (26). The lower abundance of specific *Lactobacillus sp.* might inherently predispose *Gucy2c*$^{-/-}$ mice to *Salmonella* infection, and contribute to the higher degree of translocation and epithelial damage in the ileum.

Microbiota dysbiosis has been reported in mice null for genes involved in fluid-ion homeostasis of the gut (51, 52). It is possible that GC-C enhances growth and colonization of *Lactobacillus sp.* in the gut by providing and maintaining the luminal pH and/or electrolyte distribution and balance. Certain species of *Lactobacillus* have been shown to produce indole-3-aldehyde that is an Ahr ligand. (49). Metagenomic analysis of the microbiome of

311 *Gucy2c*$^{-/-}$ mice may reveal another mechanism by with reduced levels of specific *Lactobacilli*
312 could affect IL-22 production in an AhR-dependent manner.

313 In summary, we have studied the role of GC-C during *S.* Typhimurium infection in mice and
314 have identified GC-C as a crucial host factor that provides protection against gut-mediated
315 infection by *S.* Typhimurium. Our results, summarized in Fig. 7, indicate that *Salmonella*
316 infection results in downregulation of GC-C ligands and a modest but significant
317 downregulation of GC-C. Absence of GC-C in the gut modulates the innate immune response
318 to *Salmonella* and cytokine production, possibly affecting neutrophil migration and/or stem
319 cell proliferation in the distal ileum. We speculate, therefore, that administration of GC-C
320 ligand analogs may alleviate *Salmonella*-mediated symptoms and pathology. Linaclotide is a
321 FDA approved oral GC-C ligand and is used in treatment of constipation and chronic
322 idiopathic constipation. This drug is effective against visceral pain associated with
323 constipation predominant inflammatory bowel syndrome (C-IBS) (53). Therefore,
324 paradoxically, a target for a bacterial toxin that causes diarrhoea may act as a therapeutic
325 target for treatment and alleviation of *Salmonella*-mediated intestinal symptoms and
326 pathology.

327 **Materials and Methods**

328 **Bacterial cultures**

329 The *S.* Typhimurium NCTC 12023 strain was used for mice infections. A single isolated
330 colony of *S.* Typhimurium grown on a *Salmonella-Shigella* (SS) agar plate was used to grow
331 culture the pre-inoculum. The overnight pre-inoculum was used at 0.2% in 50 mL of Luria
332 broth and cultured for 3 hours at 37°C and 160 rpm to obtain a log phase culture. The
333 bacterial culture was washed and resuspended in sterile phosphate-buffered saline (PBS) and
334 used for infection (21).

335 **Mice**

336 *Gucy2c*$^{-/-}$ obtained from the Jackson laboratory, were backcrossed with C57BL/6 mice for
337 more than 10 generations with multiple founder wild type mice. *Gucy2c*$^{+/+}$ and *Gucy2c*$^{-/-}$
338 mice were bred in the same vivarium, as described previously (15), and housed in a clean air
339 facility in multiple cages, separated based on sex and strain. Temperature (22 ± 2°C) and
340 humidity (55 ± 10%) were maintained with a 12 h light/dark cycle. Mice had access to
341 laboratory chow and water *ad libitum*. Chow was procured from Rayans Biotech, Hyderabad,
342 India, and contained ~ 24% protein, 6% oil, and 3% dietary fiber. Mice aged 6-8 weeks of
343 either sex, weighing 18-30 grams were used for experiments, and following infection housed
344 in multiple cages to rule out cage-dependent effects.

345 In some experiments, *Gucy2c*$^{-/-}$mice, at the time of weaning, were co-housed with adult wild
346 type mice for 4 weeks in multiple cages. Feces were collected from co-housed *Gucy2c*$^{-/-}$
347 mice, and mice then placed in a cage along with the wild type mice to be used for infection.
348 Three days later, mice were used for infection.

349 **Ethics statement**

350 The experiments were performed in agreement with the Control and Supervision rules, 1998
351 of Ministry of Environment and Forest Act (Government of India) and the Institutional
352 Animal Ethics Committee of the Indian Institute of Science (IISc). *Gucy2c*$^{+/+}$ and *Gucy2c*$^{-/-}$
353 mice were bred and maintained at the Central Animal Facility of IISc (Registration number:
354 48/1999/CPCSEA, dated 1/3/1999). The experimental protocols were approved by the
355 'Committee for Purpose and Control and Supervision of Experiments on Animals'
356 (CPCSEA), permit number: CAF/Ethics/216/2011. The details of the national guidelines can
357 be found on: http://envfor.nic.in/division/committee-purpose-control-and-supervision-
358 experiments-animals-cpcsea (21).

359 **Mice infection**

360 The mice were infected with *S.* Typhimurium either orally or intra-peritoneally and survival
361 was monitored. For infections via the intra-peritoneal route, ~750 bacteria/mouse were
362 administered, while for oral infection, ~10^8 bacteria/mouse were used. The bacterial culture
363 was resuspended in PBS and 0.5 mL was administered either intraperitoneally or by oral
364 gavage.

365 Fresh fecal samples were collected following infection, weighed, homogenized in PBS and
366 the appropriate dilutions were plated on SS agar plates. For quantification of CFU burden in
367 organs, the mice were sacrificed at the indicated time points and the organs were harvested,
368 weighed and homogenized in PBS. Appropriate dilutions were plated on SS agar plates (20).

369 **Serum cytokines and cortisol estimation**

370 Serum TNF-α, IL-6 and IFN-γ were quantified using ELISA kits (eBioscience, USA), while
371 serum cortisol amounts were measured using the AccuBind ELISA kit (Monobind Inc., USA)
372 according to the manufacturer's instructions (21).

373 **Flow cytometric analysis of thymocytes**

374 On indicated days, uninfected and infected mice were sacrificed, thymi dissected and washed
375 in PBS. The organs were disrupted with a pair of forceps and the cell suspensions were
376 passed through a fine wire mesh to obtain a single cell suspension, and viability of the cells
377 was estimated by Trypan blue exclusion assay using a haemocytometer. Thymocytes were
378 stained for cell surface expression of CD4 and CD8 to estimate the major cell subpopulations.
379 Anti-mouse CD4-APC (17-0041-83) and anti-mouse CD8-PE (12-0081-85) were purchased
380 from eBioscience. Cells were incubated with fluorochrome-conjugated antibodies at 4°C for
381 45 mins. Subsequently, the cells were washed twice with PBS and fixed in 0.5%

paraformaldehyde. The cells were acquired on the FACSVerse™ flow cytometer (BD Bioscience USA). Baseline instrument application and compensation settings were set using unstained and single stained samples respectively. Single events were gated on the basis of forward scatter-area versus forward scatter-height, while live events were gated on the basis of forward scatter-area versus side scatter-area. These selections were considered to exclusively analyse single live events. CD4 versus CD8 density plots were constructed for thymocytes and the major cell populations were quantified. WinMDI and FlowJo (9.8.5) software were used to plot and analyse the results (21).

Histological analysis

Histological analysis was performed on ileal sections, which were fixed in 4% paraformaldehyde in PBS (pH 6.9) and Periodic Acid Schiff (PAS) staining was performed (48). Briefly, following fixation, sections were dehydrated by serial immersion in increasing concentrations of ethanol and finally in paraffin. The tissues were embedded in paraffin and 4 µm sections were obtained using a microtome (Leica Biosystems, Germany). The sections were dewaxed and rehydrated by serial immersion in decreasing concentrations of ethanol. Sections were stained with PAS (Avinash Chemicals, Bangalore, India) following the manufacturer's instructions. The nuclei were subsequently stained with hematoxylin (Sigma-Aldrich, USA). Sections were then dehydrated and mounted. The sections were observed using an Olympus XI81 microscope (Olympus Corporation Tokyo, Japan).

RNA isolation and quantitative real time PCR analysis

A portion of the distal ileum was isolated and stored in TRI reagent (RNAiso Plus, TaKaRa). The RNA was isolated using the QIAGEN RNeasy kit, according to manufacturer's protocol and 4 µg of RNA was reverse transcribed to cDNA using Revert Aid reverse transcriptase (Thermo-Scientific, USA). Real-time PCR was performed using SYBR® Premix Ex Taq™

406 (Tli RNaseH Plus) on a CFX96 Touch™ Real-Time PCR Detection System (BIO-RAD,
407 USA). Three housekeeping genes Glyceraldehyde 3-phosphate dehydrogenase (*Gapdh*),
408 TATA box binding protein (*Tbp*) and β-actin (*Actb*) were used for internal normalization
409 controls. Since all three genes showed equivalent results, *Gapdh* was used for subsequent
410 normalization of the real time PCR data. Data is expressed as $2^{-\Delta CT}$. The sequences of
411 primers used for quantitative real-time PCR were obtained from those validated at the
412 PrimerBank database and are available on request (54–56).

413 **Quantitative real-time PCR amplification of 16S sequences of fecal microbiota**

414 Bacterial DNA was isolated from fecal pellets using the QIAamp® DNA Stool Mini Kit
415 according to manufacturer's instructions. The abundance of total bacteria and specific
416 intestinal bacterial phylum, class and species was quantified by real-time PCR analysis by
417 SYBR® Premix Ex Taq™ (Tli RNaseH Plus) on a StepOnePlus real-time PCR machine
418 (Applied Biosystems, USA) using 16S primers published earlier (57, 58) . The efficiencies of
419 each primer were estimated (data not shown) and were found to be > 90%. Relative bacterial
420 abundance was determined using the ΔΔCt method by employing universal primers for 16s
421 rDNA for normalization (59). The mean of ΔΔCt values obtained for each Phyla seen in wild
422 type mice was calculated, and this value was used to express the fold-change in individual
423 ΔΔCt values for wild type and *Gucy2c*$^{-/-}$ mice, to obtain the data shown in Fig. 6.

424 **Statistical analysis**

425 All data was analysed using GraphPad Prism 7. The pooled results from independent
426 experiments are depicted as mean ± SD. All data was tested for normality distribution by the
427 Shapiro-Wilk normality test and found to be normally distributed. Statistical significance
428 among groups of mice were determined using two-way ANOVA, with multiple comparisons,
429 and FDR by the two-stage linear step-up procedure of Benjamini, Krieger and Yekutieli.

Students t-test with 95% confidence interval was used for comparing abundance of microbiota in fecal samples. Statistical significance between the mice survival curves were obtained by the Gehan-Breslow-Wilcoxon test. The denoted p values are as follows: *p<0.05, **p<0.01, ***p<0.001.

Acknowledgements

The authors acknowledge facilities provided by the Central Animal Facility at the Indian Institute of Science for housing mice. Financial support from the Department of Biotechnology (DBT), Government of India (SSV) is acknowledged, as well as support provided to the Division of Biological Sciences in the form of Grant-In-Aid by DBT. SSV is a JC Bose National Fellow and support from the Department of Science and Technology, Government of India, is acknowledged. SSV is a recipient of a Royal Society International Collaboration Award for Research Professors along with Prof. Gad Frankel from Imperial College London. SSV would like to thank Prof. Gad Frankel and Dr. Avinash R. Shenoy in the Centre for Molecular Bacteriology and Infection at Imperial College, London, for useful discussions.

References

1. Santos RL, Raffatellu M, Bevins CL, Adams LG, Tukel C, Tsolis RM, Baumler AJ. 2009. Life in the inflamed intestine, Salmonella style. Trends Microbiol 17:498–506.

2. Hapfelmeier S, Hardt WD. 2005. A mouse model for S. typhimurium-induced enterocolitis. Trends Microbiol 13:497–503.

3. Stecher B, Paesold G, Barthel M, Kremer M, Jantsch J, Stallmach T, Heikenwalder M, Hardt WD. 2006. Chronic Salmonella enterica serovar Typhimurium-induced colitis and cholangitis in streptomycin-pretreated Nramp1+/+ mice. Infect Immun 74:5047–

5057.

4. Bao S, Beagley KW, France MP, Shen J, Husband AJ. 2000. Interferon-gamma plays a critical role in intestinal immunity against Salmonella typhimurium infection. Immunology 99:464–472.

5. Arnold JW, Niesel DW, Annable CR, Hess CB, Asuncion M, Cho YJ, Peterson JW, Klimpel GR. 1993. Tumor necrosis factor-alpha mediates the early pathology in Salmonella infection of the gastrointestinal tract. Microb Pathog 14:217–227.

6. Arnold JW, Klimpel GR, Niesel DW. 1993. Tumor necrosis factor (TNF alpha) regulates intestinal mucus production during salmonellosis. Cell Immunol 151:336–344.

7. Sadik CD, Kim ND, Luster AD. 2011. Neutrophils cascading their way to inflammation. Trends Immunol 32:452–460.

8. Zhou D, Galan J. 2001. Salmonella entry into host cells: the work in concert of type III secreted effector proteins. Microbes Infect 3:1293–1298.

9. Currie MG, Fok KF, Kato J, Moore RJ, Hamra FK, Duffin KL, Smith CE. 1992. Guanylin: an endogenous activator of intestinal guanylate cyclase. Proc Natl Acad Sci U S A 89:947–951.

10. Hamra FK, Forte LR, Eber SL, Pidhorodeckyj N V, Krause WJ, Freeman RH, Chin DT, Tompkins JA, Fok KF, Smith CE, Duffin KL, Siegel N, Currie MG. 1993. Uroguanylin: structure and activity of a second endogenous peptide that stimulates intestinal guanylate cyclase. Proc Natl Acad Sci U S A 90:10464–10468.

11. Basu N, Arshad N, Visweswariah SS. 2010. Receptor guanylyl cyclase C (GC-C):

Regulation and signal transduction. Mol Cell Biochem 334.

12. Schulz S, Green CK, Yuen PS, Garbers DL. 1990. Guanylyl cyclase is a heat-stable enterotoxin receptor. Cell 63:941–948.

13. Schulz S, Lopez MJ, Kuhn M, Garbers DL. 1997. Disruption of the guanylyl cyclase-C gene leads to a paradoxical phenotype of viable but heat-stable enterotoxin-resistant mice. J Clin Invest 100:1590–1595.

14. Lin JE, Snook AE, Li P, Stoecker BA, Kim GW, Magee MS, Garcia A V, Valentino MA, Hyslop T, Schulz S, Waldman SA. 2012. GUCY2C opposes systemic genotoxic tumorigenesis by regulating AKT-dependent intestinal barrier integrity. PLoS One 7:e31686.

15. Basu N, Saha S, Khan I, Ramachandra SG, Visweswariah SS. 2014. Intestinal cell proliferation and senescence are regulated by receptor guanylyl cyclase C and p21. J Biol Chem 289.

16. Mann EA, Harmel-Laws E, Cohen MB, Steinbrecher KA. 2013. Guanylate cyclase C limits systemic dissemination of a murine enteric pathogen. BMC Gastroenterol 13:135.

17. Barthel M, Hapfelmeier S, Quintanilla-Martinez L, Kremer M, Rohde M, Hogardt M, Pfeffer K, Russmann H, Hardt WD. 2003. Pretreatment of mice with streptomycin provides a Salmonella enterica serovar Typhimurium colitis model that allows analysis of both pathogen and host. Infect Immun 71:2839–2858.

18. Sekirov I, Tam NM, Jogova M, Robertson ML, Li Y, Lupp C, Finlay BB. 2008. Antibiotic-induced perturbations of the intestinal microbiota alter host susceptibility to enteric infection. Infect Immun 76:4726–4736.

498 19. Ren Z, Gay R, Thomas A, Pae M, Wu D, Logsdon L, Mecsas J, Meydani SN. 2009.
499 Effect of age on susceptibility to Salmonella Typhimurium infection in C57BL/6 mice.
500 J Med Microbiol 58:1559–1567.

501 20. Deobagkar-Lele M, Chacko SK, Victor ES, Kadthur JC, Nandi D. 2013. Interferon-
502 gamma- and glucocorticoid-mediated pathways synergize to enhance death of CD4(+)
503 CD8(+) thymocytes during Salmonella enterica serovar Typhimurium infection.
504 Immunology 138:307–321.

505 21. Majumdar S, Deobagkar-Lele M, Adiga V, Raghavan A, Wadhwa N, Ahmed SM,
506 Rananaware SR, Chakraborty S, Joy O, Nandi D. 2017. Differential susceptibility and
507 maturation of thymocyte subsets during Salmonella Typhimurium infection: insights
508 on the roles of glucocorticoids and Interferon-gamma. Sci Rep 7:40793.

509 22. Ikpa PT, Sleddens HF, Steinbrecher KA, Peppelenbosch MP, de Jonge HR, Smits R,
510 Bijvelds MJ. 2016. Guanylin and uroguanylin are produced by mouse intestinal
511 epithelial cells of columnar and secretory lineage. Histochem Cell Biol 146:445–455.

512 23. Arshad N, Visweswariah SS. 2012. The multiple and enigmatic roles of guanylyl
513 cyclase C in intestinal homeostasis. FEBS Lett 586.

514 24. LaRock DL, Chaudhary A, Miller SI. 2015. Salmonellae interactions with host
515 processes. Nat Rev Microbiol 13:191–205.

516 25. Nakazato G, Paganelli FL, Lago JC, Aoki FH, Mobilon C, Brocchi M, Stehling EG,
517 Silveira WD. 2011. Lactobacillus acidophilus decreases Salmonella Typhimurium
518 invasion in vivo. J Food Saf 31:284–289.

519 26. Huang IF, Lin IC, Liu PF, Cheng MF, Liu YC, Hsieh YD, Chen JJ, Chen CL, Chang
520 HW, Shu CW. 2015. Lactobacillus acidophilus attenuates Salmonella-induced

intestinal inflammation via TGF-beta signaling. BMC Microbiol 15:203.

27. Abdel-Daim A, Hassouna N, Hafez M, Ashor MS, Aboulwafa MM. 2013. Antagonistic activity of Lactobacillus isolates against Salmonella typhi in vitro. Biomed Res Int 2013:680605.

28. Coconnier MH, Lievin V, Lorrot M, Servin AL. 2000. Antagonistic activity of Lactobacillus acidophilus LB against intracellular Salmonella enterica serovar Typhimurium infecting human enterocyte-like Caco-2/TC-7 cells. Appl Env Microbiol 66:1152–1157.

29. Nicolaides NC, Kyratzi E, Lamprokostopoulou A, Chrousos GP, Charmandari E. 2015. Stress, the stress system and the role of glucocorticoids. Neuroimmunomodulation 22:6–19.

30. Tannock GW, Blumershine R V, Savage DC. 1975. Association of Salmonella typhimurium with, and its invasion of, the ileal mucosa in mice. Infect Immun 11:365–370.

31. Stecher B, Macpherson AJ, Hapfelmeier S, Kremer M, Stallmach T, Hardt WD. 2005. Comparison of Salmonella enterica serovar Typhimurium colitis in germfree mice and mice pretreated with streptomycin. Infect Immun 73:3228–3241.

32. Caprilli R. 2008. Why does Crohn's disease usually occur in terminal ileum? J Crohn's Colitis 2:352–356.

33. Cominelli F, Arseneau KO, Rodriguez-Palacios A, Pizarro TT. 2017. Uncovering Pathogenic Mechanisms of Inflammatory Bowel Disease Using Mouse Models of Crohn's Disease-Like Ileitis: What is the Right Model? Cell Mol Gastroenterol Hepatol 4:19–32.

544 34. He P, Yun CC. 2010. Mechanisms of the regulation of the intestinal Na+/H+
545 exchanger NHE3. J Biomed Biotechnol 2010:238080.

546 35. Lan D, Niu J, Miao J, Dong X, Wang H, Yang G, Wang K, Miao Y. 2016. Expression
547 of guanylate cyclase-C, guanylin, and uroguanylin is downregulated proportionally to
548 the ulcerative colitis disease activity index. Sci Rep 6.

549 36. Brenna Ø, Bruland T, Furnes MW, Granlund AVB, Drozdov I, Emgård J, Brønstad G,
550 Kidd M, Sandvik AK, Gustafsson BI. 2015. The guanylate cyclase-C signaling
551 pathway is down-regulated in inflammatory bowel disease. Scand J Gastroenterol
552 50:1241–1252.

553 37. Pattison AM, Merlino DJ, Blomain ES, Waldman SA. 2016. Guanylyl cyclase C
554 signaling axis and colon cancer prevention. World J Gastroenterol 22:8070–8077.

555 38. Nakano Y, Onozuka K, Terada Y, Shinomiya H, Nakano M. 1990. Protective effect of
556 recombinant tumor necrosis factor-alpha in murine salmonellosis. J Immunol
557 144:1935–1941.

558 39. Tracey KJ, Beutler B, Lowry SF, Merryweather J, Wolpe S, Milsark IW, Hariri RJ,
559 Fahey 3rd TJ, Zentella A, Albert JD, Shires G, Cerami A. 1986. Shock and tissue
560 injury induced by recombinant human cachectin. Science 234:470–474.

561 40. Beutler B, Grau GE. 1993. Tumor necrosis factor in the pathogenesis of infectious
562 diseases. Crit Care Med 21:S423-35.

563 41. Zheng Y, Danilenko DM, Valdez P, Kasman I, Eastham-Anderson J, Wu J, Ouyang
564 W. 2007. Interleukin-22, a T(H)17 cytokine, mediates IL-23-induced dermal
565 inflammation and acanthosis. Nature 445:648–651.

566 42. Powell N, Lo JW, Biancheri P, Vossenkamper A, Pantazi E, Walker AW, Stolarczyk
567 E, Ammoscato F, Goldberg R, Scott P, Canavan JB, Perucha E, Garrido-Mesa N,
568 Irving PM, Sanderson JD, Hayee B, Howard JK, Parkhill J, MacDonald TT, Lord GM.
569 2015. Interleukin 6 Increases Production of Cytokines by Colonic Innate Lymphoid
570 Cells in Mice and Patients With Chronic Intestinal Inflammation. Gastroenterology
571 149:456–67 e15.

572 43. Vaishnava S, Yamamoto M, Severson KM, Ruhn KA, Yu X, Koren O, Ley R,
573 Wakeland EK, Hooper L V. 2011. The antibacterial lectin RegIIIgamma promotes the
574 spatial segregation of microbiota and host in the intestine. Science (80-) 334:255–258.

575 44. Behnsen J, Jellbauer S, Wong CP, Edwards RA, George MD, Ouyang W, Raffatellu
576 M. 2014. The cytokine IL-22 promotes pathogen colonization by suppressing related
577 commensal bacteria. Immunity 40:262–273.

578 45. van Ampting MTJ, Loonen LMP, Schonewille AJ, Konings I, Vink C, Iovanna J,
579 Chamaillard M, Dekker J, van der Meer R, Wells JM. 2012. Intestinally secreted C-
580 type lectin Reg3b attenuates salmonellosis but not listeriosis in mice. Infect Immun
581 80:1115–1120.

582 46. Loonen LM, Stolte EH, Jaklofsky MT, Meijerink M, Dekker J, van Baarlen P, Wells
583 JM. 2014. REG3gamma-deficient mice have altered mucus distribution and increased
584 mucosal inflammatory responses to the microbiota and enteric pathogens in the ileum.
585 Mucosal Immunol 7:939–947.

586 47. Lindemans CA, Calafiore M, Mertelsmann AM, O'Connor MH, Dudakov JA, Jenq
587 RR, Velardi E, Young LF, Smith OM, Lawrence G, Ivanov JA, Fu YY, Takashima S,
588 Hua G, Martin ML, O'Rourke KP, Lo YH, Mokry M, Romera-Hernandez M, Cupedo

589 T, Dow LE, Nieuwenhuis EE, Shroyer NF, Liu C, Kolesnick R, Van Den Brink MRM,
590 Hanash AM. 2015. Interleukin-22 promotes intestinal-stem-cell-mediated epithelial
591 regeneration. Nature 528:560–564.

592 48. Murray IA, Perdew GH. 2016. Ligand activation of the Ah receptor contributes to
593 gastrointestinal homeostasis. Curr Opin Toxicol.

594 49. Zelante T, Iannitti RG, Cunha C, DeLuca A, Giovannini G, Pieraccini G, Zecchi R,
595 D'Angelo C, Massi-Benedetti C, Fallarino F, Carvalho A, Puccetti P, Romani L. 2013.
596 Tryptophan catabolites from microbiota engage aryl hydrocarbon receptor and balance
597 mucosal reactivity via interleukin-22. Immunity 39:372–385.

598 50. Bäumler AJ, Sperandio V. 2016. Interactions between the microbiota and pathogenic
599 bacteria in the gut. Nature 535:85–93.

600 51. Larmonier CB, Laubitz D, Hill FM, Shehab KW, Lipinski L, Midura-Kiela MT,
601 McFadden RM, Ramalingam R, Hassan KA, Golebiewski M, Besselsen DG, Ghishan
602 FK, Kiela PR. 2013. Reduced colonic microbial diversity is associated with colitis in
603 NHE3-deficient mice. Am J Physiol Gastrointest Liver Physiol 305:G667-77.

604 52. Norkina O, Burnett TG, De Lisle RC. 2004. Bacterial overgrowth in the cystic fibrosis
605 transmembrane conductance regulator null mouse small intestine. Infect Immun
606 72:6040–6049.

607 53. Castro J, Harrington AM, Hughes PA, Martin CM, Ge P, Shea CM, Jin H, Jacobson S,
608 Hannig G, Mann E, Cohen MB, MacDougall JE, Lavins BJ, Kurtz CB, Silos-Santiago
609 I, Johnston JM, Currie MG, Blackshaw LA, Brierley SM. 2013. Linaclotide inhibits
610 colonic nociceptors and relieves abdominal pain via guanylate cyclase-C and
611 extracellular cyclic guanosine 3',5'-monophosphate. Gastroenterology 145:1311–

1334.

54. Wang X, Seed B. 2003. A PCR primer bank for quantitative gene expression analysis. Nucleic Acids Res 31:e154.

55. Spandidos A, Wang X, Wang H, Dragnev S, Thurber T, Seed B. 2008. A comprehensive collection of experimentally validated primers for Polymerase Chain Reaction quantitation of murine transcript abundance. BMC Genomics 9:633.

56. Spandidos A, Wang X, Wang H, Seed B. 2010. PrimerBank: a resource of human and mouse PCR primer pairs for gene expression detection and quantification. Nucleic Acids Res 38:D792-9.

57. Yang Y-W, Chen M-K, Yang B-Y, Huang X-J, Zhang X-R, He L-Q, Zhang J, Hua Z-C. 2015. Use of 16S rRNA gene-targeted group-specific primers for real-time PCR analysis of predominant bacteria in mouse feces. Appl Environ Microbiol 81:6749–6756.

58. Clifford RJ, Milillo M, Prestwood J, Quintero R, Zurawski D V, Kwak YI, Waterman PE, Lesho EP, Mc Gann P. 2012. Detection of bacterial 16S rRNA and identification of four clinically important bacteria by real-time PCR. PLoS One 7:e48558.

59. Feng Y, Gong J, Yu H, Jin Y, Zhu J, Han Y. 2010. Identification of changes in the composition of ileal bacterial microbiota of broiler chickens infected with Clostridium perfringens. Vet Microbiol 140:116–121.

Legends to Figures

Figure 1: *Gucy2c*$^{-/-}$ mice display accelerated mortality during oral infection with *S.* Typhimurium. (a) *Gucy2c*$^{+/+}$ and *Gucy2c*$^{-/-}$ mice were infected with *S.* Typhimuirum either orally or intra-peritoneally. The mice were monitored for survival at 8 h intervals. Survival curves for oral and intra-peritoneal infection were obtained from independent experiments containing a total of 10-11 mice. (b) Mice (*Gucy2c*$^{+/+}$, black circles; *Gucy2c*$^{-/-}$, grey circles) were orally infected with *S.* Typhimurium and the bacterial load in the feces on day 1 and 2 following infection were estimated. Data show values for individual mice, with error bars showing the mean ± SD. (c) Infected mice were sacrificed on day 3, tissues harvested and bacterial burden in the spleen, Peyer's patches and liver was estimated. Data show values for individual mice, with error bars showing the mean ± SD. (d) Mice were weighed prior to oral infection and 3 days post infection. (e) Serum was collected from uninfected and infected mice and levels of TNF-α, IFN-γ and IL-6 were measured by ELISA. In panels b-e, the data are depicted as mean ± SD of 3-7 mice per group. Statistical significance among the experimental groups in all panels was analysed using two-way ANOVA, *$p \leq 0.05$ and ns: not significant.

Figure 2. Early rise in serum cortisol amounts and increased infection-induced thymic atrophy is observed in *Gucy2c*$^{-/-}$ mice. (a) *Gucy2c*$^{+/+}$ and *Gucy2c*$^{-/-}$ mice were orally infected with *S.* Typhimurium. At the indicated time points, uninfected (-St) and infected (+St) mice were sacrificed and serum cortisol levels were measured by ELISA. Data show values for individual mice, with error bars showing the mean ± SD. (b) Viable cells from harvested thymi were quantified by Trypan blue exclusion assay using a haemocytometer. (c) The thymocytes from uninfected (-St) and mice post 96 h of infection (+St) were stained for

656 cell surface expression of CD4 and CD8 and the density plots were constructed to quantify
657 the percentages of the major cell populations. Data are depicted as mean ± SEM of 5-8 mice
658 per group. In all panels, experimental groups were analysed for statistical significance using
659 two-way ANOVA, *$p \leq 0.05$, ***$p \leq 0.001$ and ****$p \leq 0.0001$. Green bars indicate
660 differences that were statistically significant between *Gucy2c*$^{+/+}$ (black circles) and *Gucy2c*$^{-/-}$
661 (grey circles) mice.

662

663 **Figure 3: *Gucy2c*$^{-/-}$ mice show increased bacterial colonization and intestinal damage.**
664 Infected *Gucy2c*$^{+/+}$ (black circles) and *Gucy2c*$^{-/-}$ (grey circles) mice were sacrificed 3 days
665 post oral *S.* Typhimurium infection. (a) Bacterial load in the ileum, cecum and colon was
666 estimated. Values represent individual mice, and lines show the mean ± SD. (b) Periodic
667 Acid Schiff (PAS) staining was performed on formalin fixed ileal tissue sections obtained
668 from uninfected (-St) and infected (+St) on day 3 and 4 following infection. One
669 representative ileal tissue section from each experimental group containing 3-4 mice is
670 depicted, and the scale bars measure 100 μm. Arrow shows a large number of apoptic cells in
671 the lumen of *Gucy2c*$^{-/-}$ mice. (c) The number of goblet cells was quantified in individual,
672 clearly identifiable, villi in each section from uninfected (–St; black circles) and infected
673 (+St; red circles) mice. Data shown is from individual villi across a section, and lines indicate
674 the mean ± SD. Statistical analysis was performed by two-way ANOVA and *$p \leq 0.05$.

675

676 **Figure 4. *S.* Typhimurium infection regulates expression of genes in the GC-C signaling**
677 **pathway.** RNA was prepared from ileal tissue of uninfected (-St) and infected (+St) mice on
678 day 3 following oral infection. Quantitative real-time PCR analysis was performed to
679 estimate the transcript levels of *Gucy2c, Guca2a, Guca2b, PkgII, Pde5, Nhe3 and Cftr*. The

680 data are depicted as values for individual mice, and lines represent the mean ± SD. Two-way
681 ANOVA was used to analyse for statistical significance among the experimental groups, *$p \leq$
682 0.05, **$p \leq 0.01$, ***$p \leq 0.001$ and ns: not significant.

683

684 **Figure 5. *Gucy2c*$^{-/-}$ mice show reduced transcript levels of IL-23/IL-22 in the ileum**
685 **following infection.** Orally infected *Gucy2c*$^{+/+}$ and *Gucy2c*$^{-/-}$ mice were sacrificed 3 days
686 post infection (+St) along with the control uninfected mice (-St). RNA was isolated from the
687 harvested ileal tissues and quantitative real-time PCR analysis was performed to estimate the
688 transcript levels of *Tnf-α, Il-1b, Il-6, Cxcl-15, Il-22, Il-23, Ifn-γ, Il-4, Cxcl-1, Cxcl-2, Cxcl-9,*
689 *Cxcl-10, Lcn 2, Reg3β* and *Reg3γ.* The data shown are from individual mice and lines depict
690 the mean ± SD. The experimental groups were analysed for statistical significance using two-
691 way ANOVA, *$p \leq 0.05$, **$p \leq 0.01$, ***$p \leq 0.001$ and ns: not significant. Green bars
692 represent values which differed significantly between *Gucy2c*$^{+/+}$ and *Gucy2c*$^{-/-}$ mice.

693

694 **Figure 6. Abundance of major microbial phyla in *Gucy2c*$^{+/+}$ and *Gucy2c*$^{-/-}$ mice.** (a) Fecal
695 pellets from uninfected *Gucy2c*$^{+/+}$ and *Gucy2c*$^{-/-}$ mice, and *Gucy2c*$^{-/-}$ mice co-housed with
696 wild type mice, were collected and the bacterial DNA was isolated from the samples.
697 Quantitative real-time PCR was performed to analyse levels of gut microbiota using Phyla
698 specific primers, normalized to universal 16S primers. Values shown represent individual
699 mice and lines show the mean ± SD. Statistical analysis was performed using non-parametric
700 Mann-Whitney *U* test, **$p \leq 0.01$. (b) *Gucy2c*$^{+/+}$ and co-housed *Gucy2c*$^{-/-}$ (4 each) were
701 infected with St and housed together in multiple cages during the course of infection.
702 Survival of mice was checked every 8h. (c) Fecal pellets from individual mice were collected
703 24 h and 48 h following infection of mice (*Gucy2c*$^{+/+}$, black circles; *Gucy2c*$^{-/-}$, grey circles)

and the bacterial load in the feces on day 1 and 2 following infection were estimated. Data show values for individual mice, with error bars showing the mean ± SD. (c) Individual mice were weighted prior to infection and then every day following infection till day 3 (when *Gucy2c*$^{-/-}$ mice had started to succumb to infection). Data shown is the mean ± SD (n=4).

Figure 7. Putative role of GC-C during Salmonella infection. The IL23/IL22 arm of the innate immune response during *Salmonella* infection is regulated by GC-C. Post oral infection in mice, *Salmonella* competes with the commensal *Lactobacillus* to invade the epithelial and dendritic cells of the gut. *Salmonella* downregulates the expression of the GC-C receptor and its endogenous ligands, guanylin and urouanylin. Probable interaction of GC-C with dendritic cells and macrophages along with IL-6 upregulation leads to induction of IL-23 expression, which activates the TH17 cells to express the cytokine IL-22, which in turn induces the expression of the AMP, Reg3β, in epithelial cells.

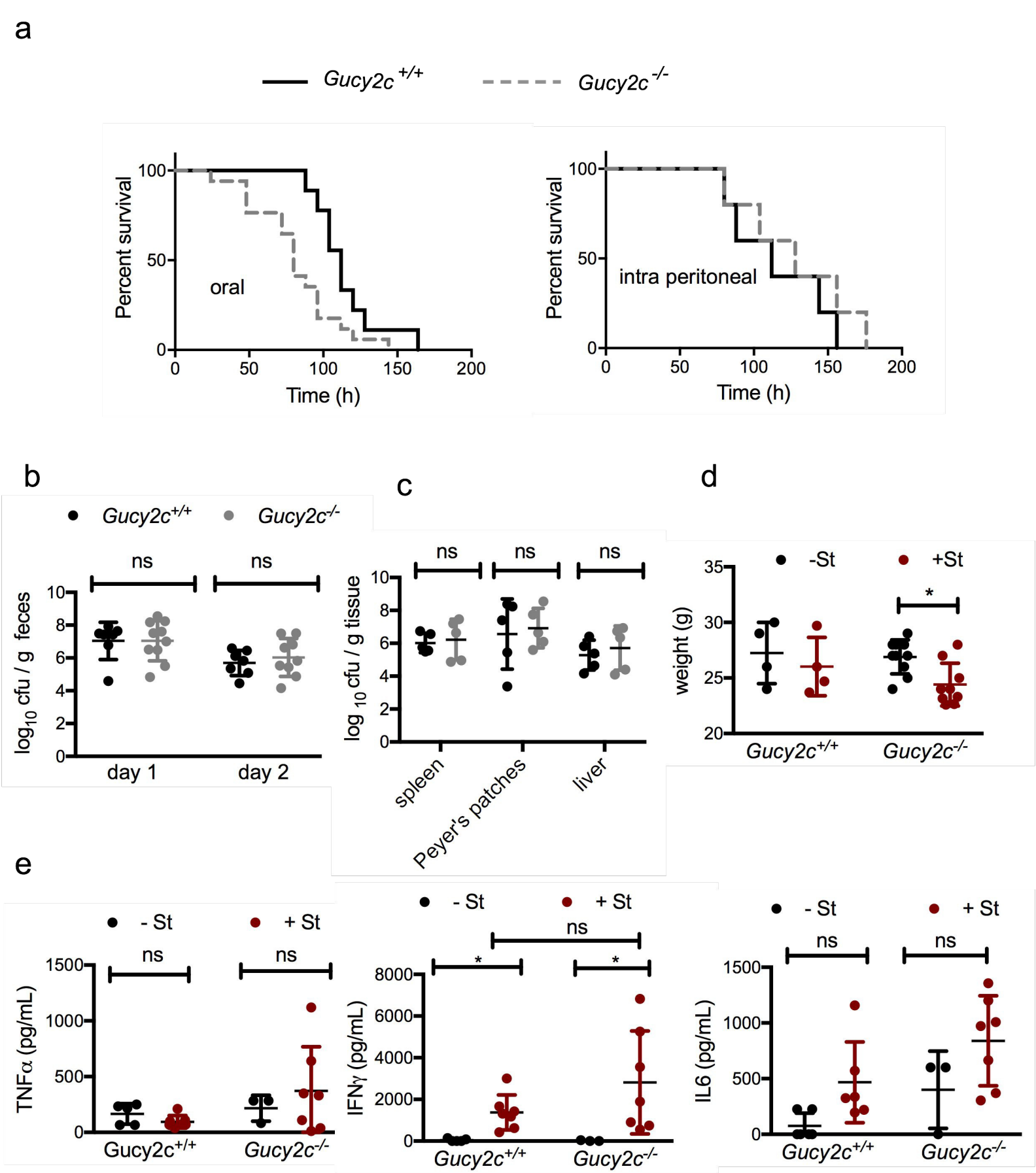
a
Gucy2c +/+
Gucy2c -/-
Percent survival
oral
Time (h)
intra peritoneal
b
Gucy2c+/+
Gucy2c-/-
ns
log10 cfu / g feces
day 1
day 2
c
log 10 cfu / g tissue
spleen
Peyer's patches
liver
d
-St
+St
weight (g)
e
- St
+ St
TNFα (pg/mL)
IFNγ (pg/mL)
IL6 (pg/mL)

Figure 1

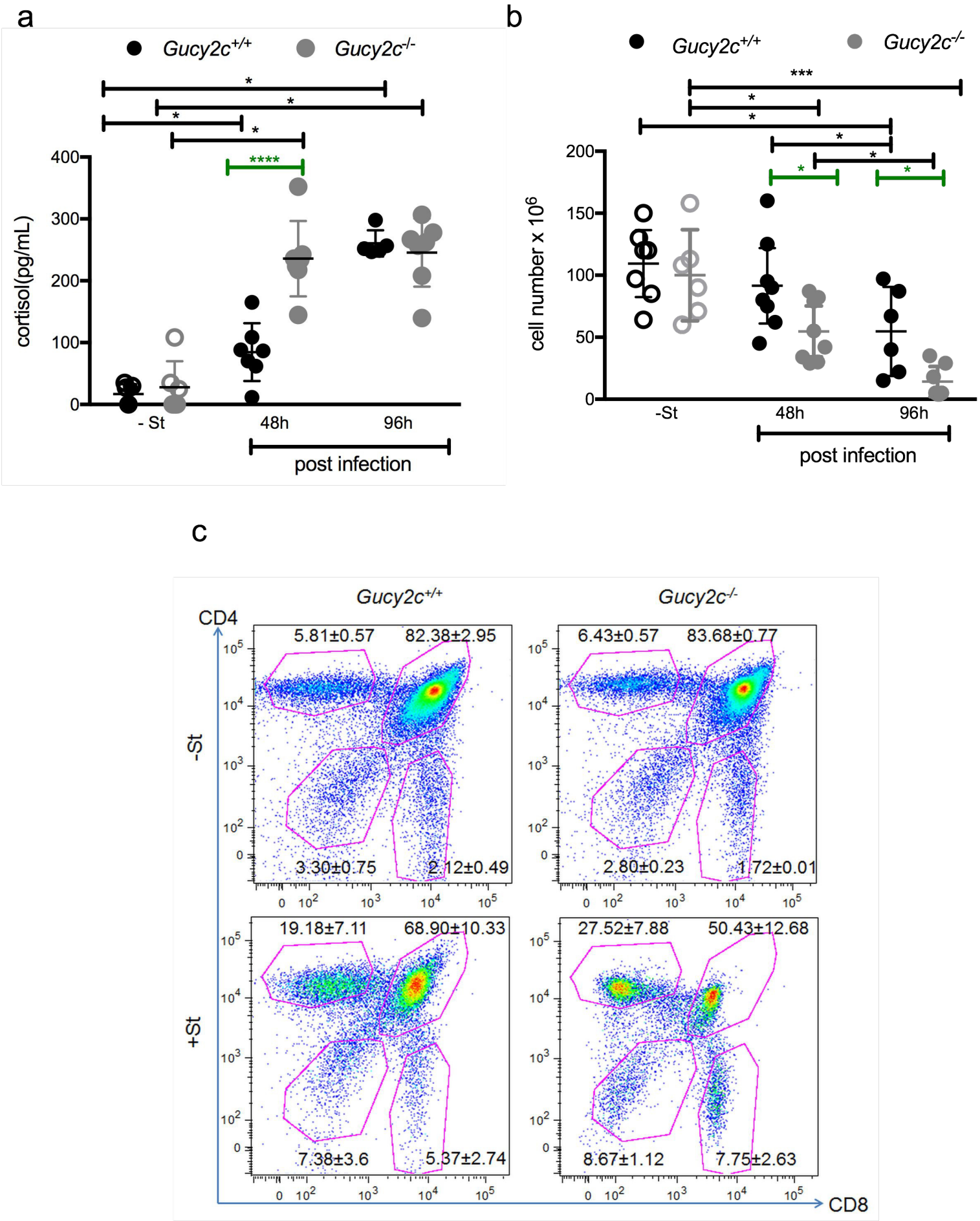
a
Gucy2c+/+
Gucy2c-/-
cortisol(pg/mL)
400
300
200
100
0
****
- St
48h
96h
post infection
b
Gucy2c+/+
Gucy2c-/-
***
cell number x 10^6
200
150
100
50
0
-St
48h
96h
post infection
c
Gucy2c+/+
Gucy2c-/-
CD4
-St
+St
CD8
5.81±0.57
82.38±2.95
3.30±0.75
2.12±0.49
6.43±0.57
83.68±0.77
2.80±0.23
1.72±0.01
19.18±7.11
68.90±10.33
7.38±3.6
5.37±2.74
27.52±7.88
50.43±12.68
8.67±1.12
7.75±2.63

Figure 2

a

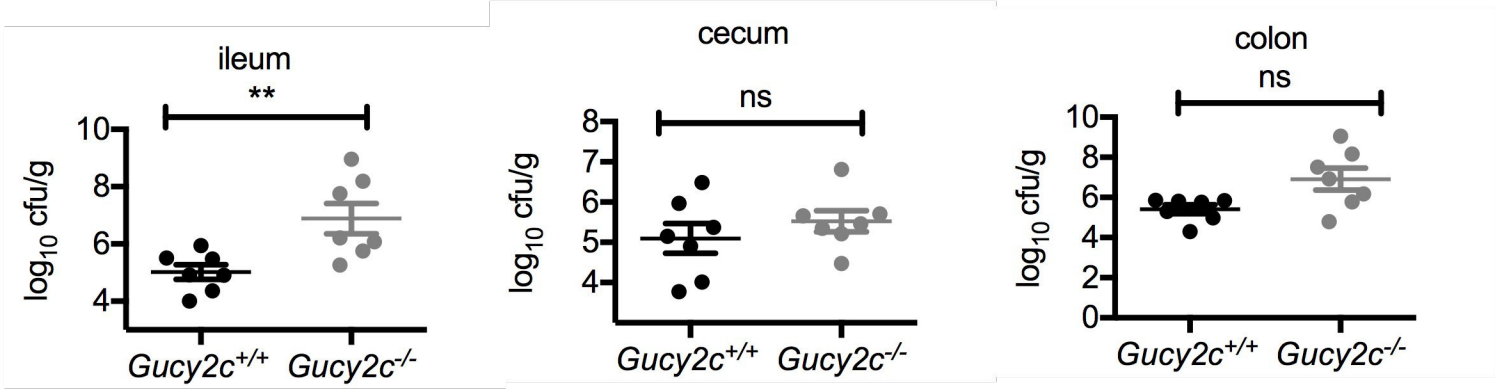
ileum
**
log10 cfu/g
10
8
6
4
Gucy2c+/+
Gucy2c-/-
cecum
ns
log10 cfu/g
8
7
6
5
4
Gucy2c+/+
Gucy2c-/-
colon
ns
log10 cfu/g
10
8
6
4
2
0
Gucy2c+/+
Gucy2c-/-

b

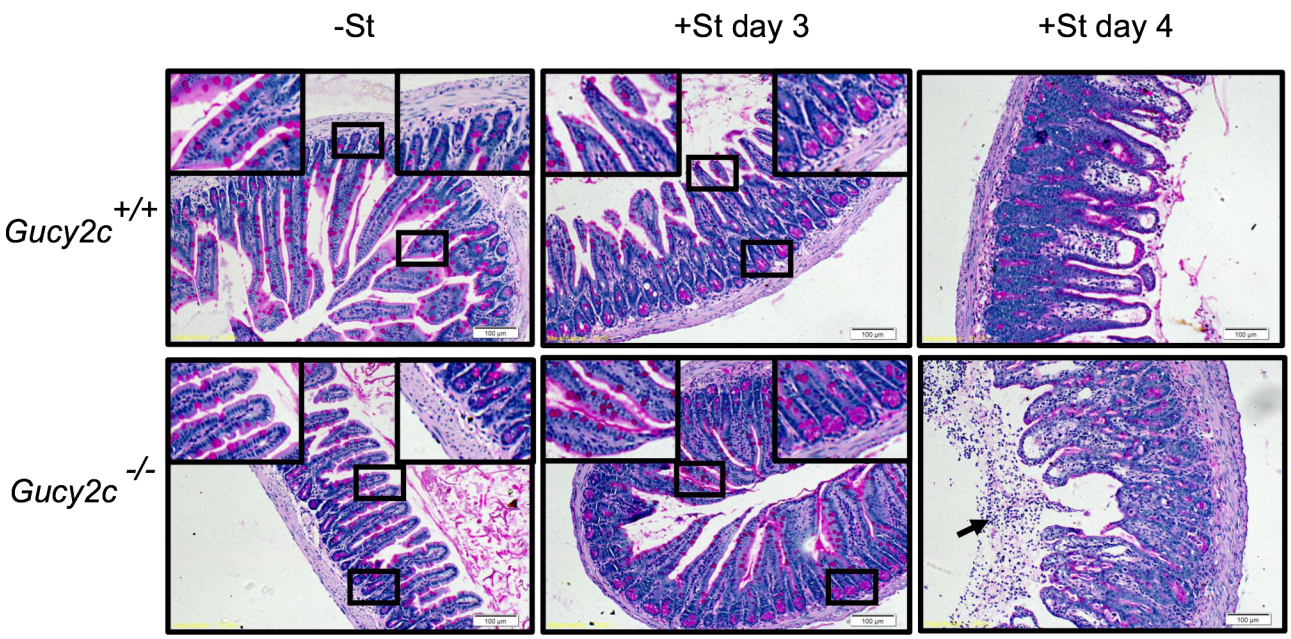
-St
+St day 3
+St day 4
Gucy2c +/+
Gucy2c -/-

c

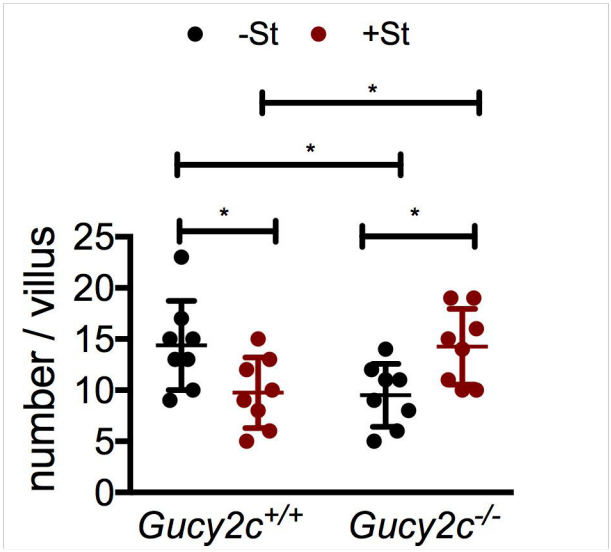
-St
+St
*
*
*
*
number / villus
25
20
15
10
5
0
Gucy2c+/+
Gucy2c-/-

Figure 3

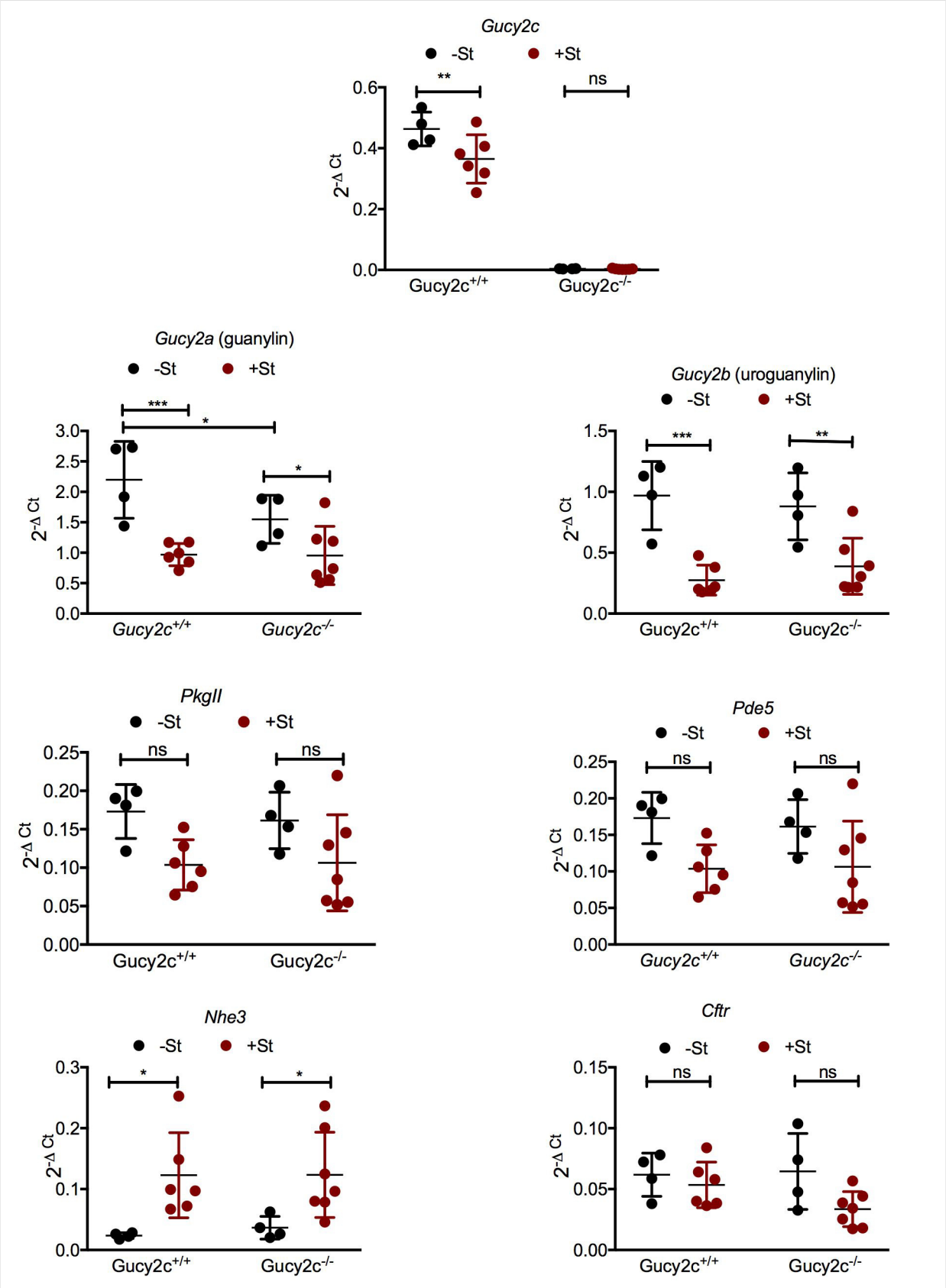
Gucy2c
-St
+St
**
ns
0.6
0.4
0.2
0.0
2-Δ Ct
Gucy2c+/+
Gucy2c-/-
Gucy2a (guanylin)
-St
+St
***
*
*
3.0
2.5
2.0
1.5
1.0
0.5
0.0
2-Δ Ct
Gucy2c+/+
Gucy2c-/-
Gucy2b (uroguanylin)
-St
+St
***
**
1.5
1.0
0.5
0.0
2-Δ Ct
Gucy2c+/+
Gucy2c-/-
PkgII
-St
+St
ns
ns
0.25
0.20
0.15
0.10
0.05
0.00
2-Δ Ct
Gucy2c+/+
Gucy2c-/-
Pde5
-St
+St
ns
ns
0.25
0.20
0.15
0.10
0.05
0.00
2-Δ Ct
Gucy2c+/+
Gucy2c-/-
Nhe3
-St
+St
*
*
0.3
0.2
0.1
0.0
2-Δ Ct
Gucy2c+/+
Gucy2c-/-
Cftr
-St
+St
ns
ns
0.15
0.10
0.05
0.00
2-Δ Ct
Gucy2c+/+
Gucy2c-/-

Figure 4

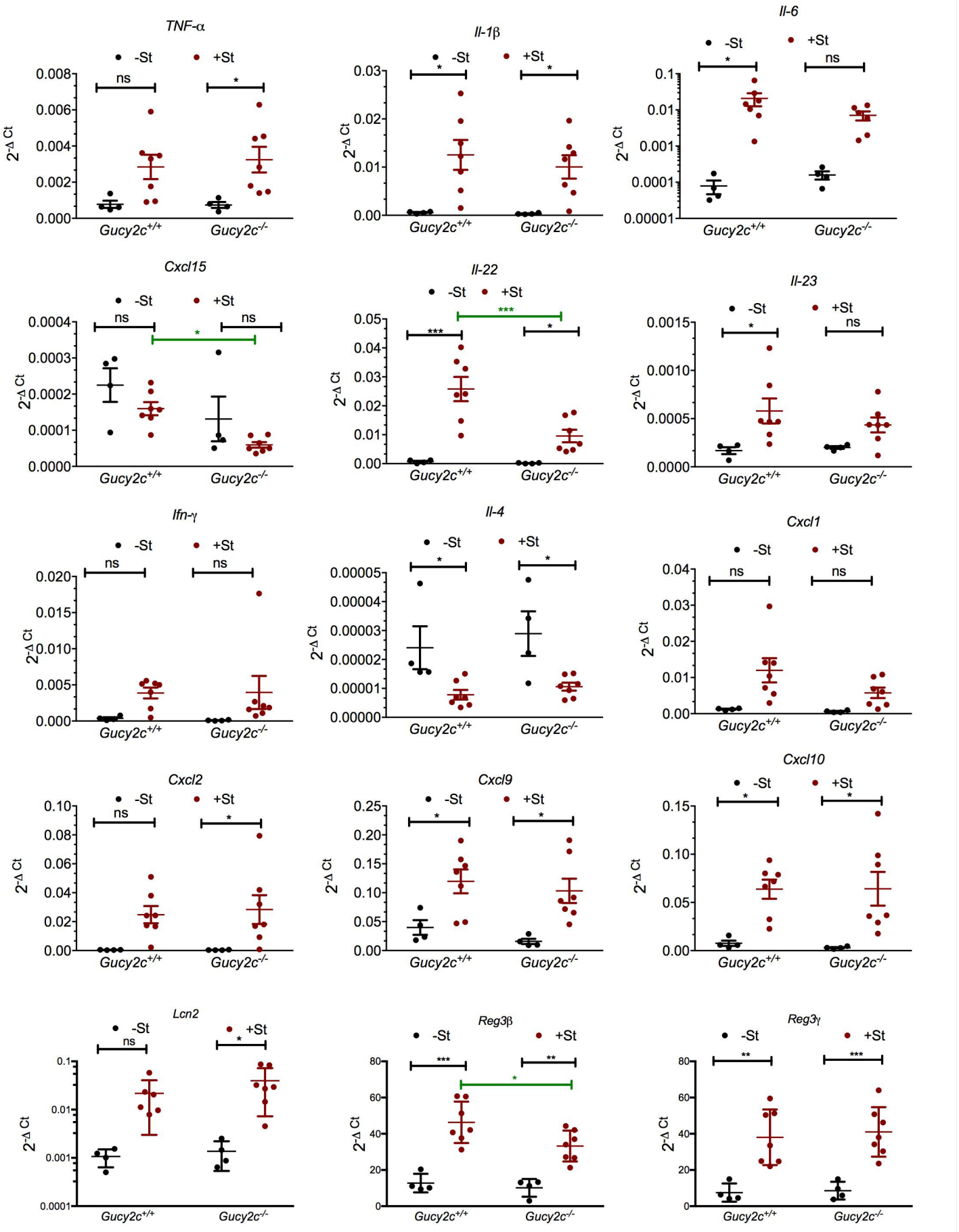
TNF-α
Il-1β
Il-6
Cxcl15
Il-22
Il-23
Ifn-γ
Il-4
Cxcl1
Cxcl2
Cxcl9
Cxcl10
Lcn2
Reg3β
Reg3γ
-St
+St
ns
2-Δ Ct
Gucy2c+/+
Gucy2c-/-

Figure 5

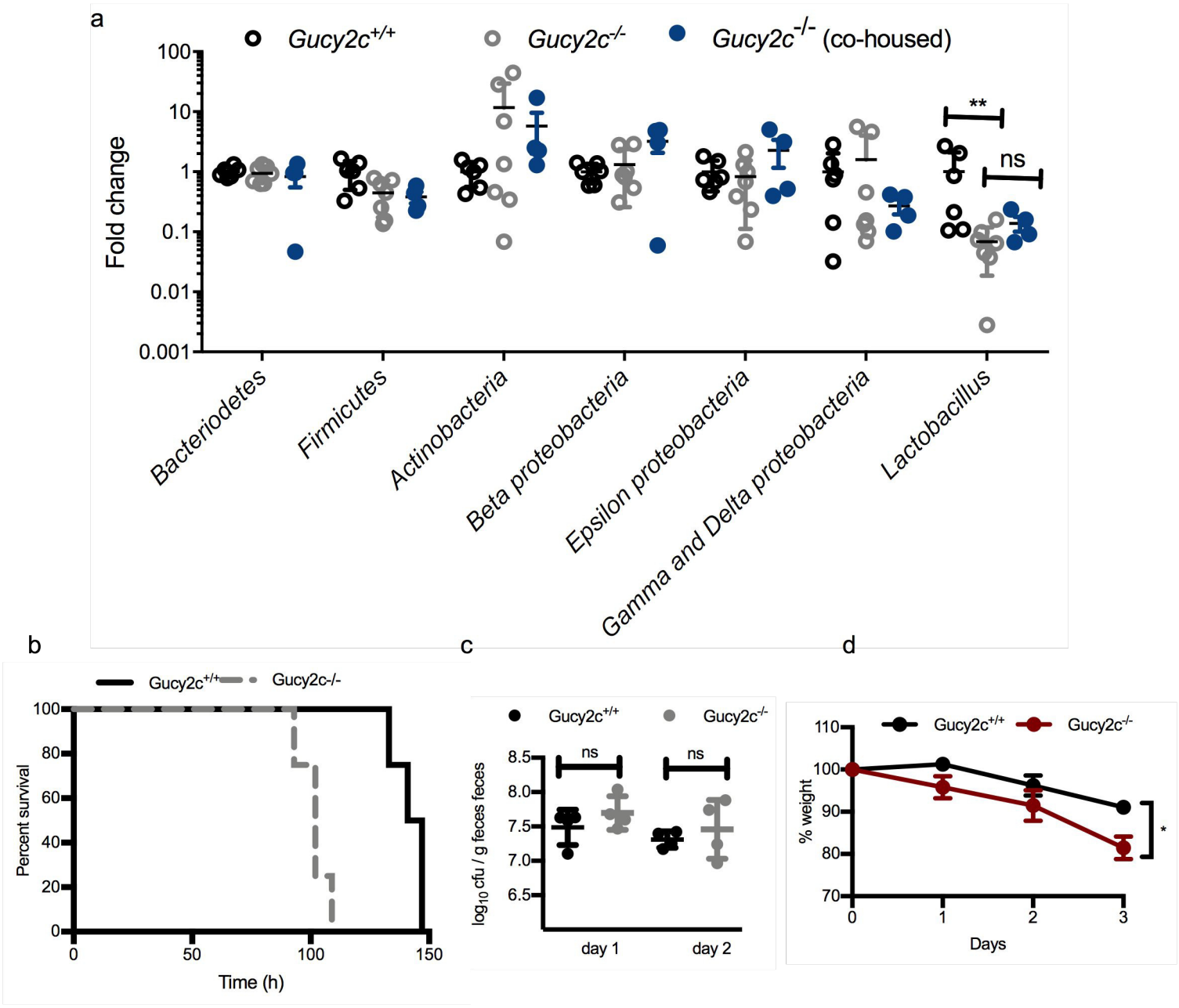
a
Gucy2c+/+
Gucy2c-/-
Gucy2c-/- (co-housed)
Fold change
100
10
1
0.1
0.01
0.001
**
ns
Bacteriodetes
Firmicutes
Actinobacteria
Beta proteobacteria
Epsilon proteobacteria
Gamma and Delta proteobacteria
Lactobacillus
b
Gucy2c+/+
Gucy2c-/-
Percent survival
100
80
60
40
20
0
0
50
100
150
Time (h)
c
Gucy2c+/+
Gucy2c-/-
log10 cfu / g feces feces
8.5
8.0
7.5
7.0
6.5
ns
ns
day 1
day 2
d
Gucy2c+/+
Gucy2c-/-
% weight
110
100
90
80
70
0
1
2
3
Days
*

Figure 6

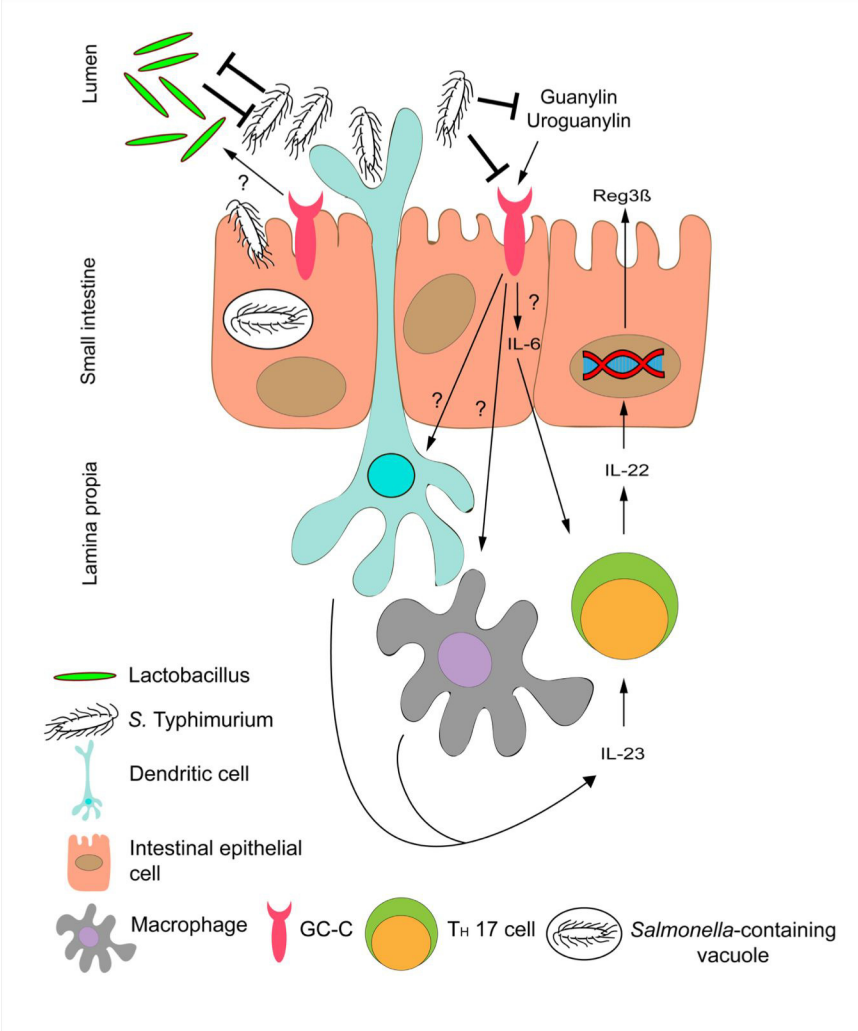
Lumen
Small intestine
Lamina propia
Guanylin
Uroguanylin
Reg3ß
IL-6
IL-22
IL-23
?
Lactobacillus
S. Typhimurium
Dendritic cell
Intestinal epithelial cell
Macrophage
GC-C
TH 17 cell
Salmonella-containing vacuole

Figure 7